World Applied Sciences Journal 12 (8): 1214-1225, 2011
ISSN 1818-4952

Free Vibration Analysis of Cracked Functionally Graded Material Beam

M. Eftekhari, M. Javadi and R.E. Farsani

Department of Mechanical Engineering, Faculty of Engineering,
Islamic Azad University, South Tehran Branch, Iran

Abstract: This paper presents an analytical model of cracked cantilevered beams made of functionally graded materials (FGMs). The local flexibility concept is implemented to model the open crack. Therefore, the open edge crack is modeled as a massless elastic rotational spring. Also, the FGM beam is formulated based on Bernoulli-Euler beam theory. It is assumed that the material properties vary along the beam thickness only according to exponential distributions. Governing equations of motion and boundary conditions are derived via the Hamilton's variational principle. Then free vibration analysis of the cracked FGM beam is presented. The results indicate that variation of natural frequencies and the corresponding mode shapes in the presence of a crack is affected by the crack ratio and location, as well as the material properties.

Key words: Cantilever beam · FGM · Free vibration · Crack

INTRODUCTION

Cracks in a structure and the associated frequency analysis are real engineering problems in many fields. Also, Understanding the dynamic characteristics of cracked structures is of prime importance in structural health monitoring. A large number of investigations in the free vibration of cracked beams are available in open literature.

Kirshmer [1], Thomson [2] and Petroski [3,4] studied the effects of crack on the vibration characteristics of cracked beams. Dimarogonas and Chondros [5-8] modeled the crack as a local flexibility computed with fracture mechanics methods. Yokoyama and Chen [9] obtained the vibration characteristics of a Bernoulli-Euler beam with a single edge crack based on a modified line-spring model. By using the differential quadrature method and the spring model, Hsu [10] studied the flexural vibration and dynamic response of edge-cracked Bernoulli-Euler beams resting on an elastic foundation and subjected to an axial loading and lateral excitation force.

Rizos *et al.* [11] modeled the crack as the local flexibility and used a semi-analytical way to correlate the measured modes with the crack location and size. Narkis [12] simulated cracks as an equivalent rotational spring and studied the dynamics and identification problems of a cracked, simply supported uniform beam.

In recent years, functionally graded materials (FGMs) have received considerable attention. FGMs have been extensively used for many applications, such as aerospace structures and high-speed turbine machinery. Sankar and Tzeng [13] obtained an analytical solution for FG simply supported Euler-Bernoulli beams subjected to temperature gradients. Wu *et al.* [14] obtained the closed form natural frequencies of a simply supported FGM beam with mass density and Young's modulus being polynomial functions of the axial coordinate. Rotating FGM thin-walled beams operating in a high-temperature environment was studied by Librescu *et al.* [15]. The free and forced vibration of a laminated functionally graded beam of variable thickness under thermally induced initial stresses by using Timoshenko beam theory was studied by Xiang and Yang [16]. Free vibration characteristics and the dynamic behavior of a functionally graded simply-supported beam under a concentrated moving harmonic load was analyzed by Simsek and Kocatürk [17].

According to the best of the authors' knowledge, in the available literature, free vibration analysis of a functionally graded cantilever beam containing an edge crack through analytical method have not yet been presented. Therefore this study is devoted to this topic.

Corresponding Author: M. Eftekhari, Department of Mechanical Engineering,
Faculty of Engineering, Islamic Azad University, South Tehran Branch, Iran.
Mob: +98-9133478964, E-mail: malihe_eftekhari@yahoo.com

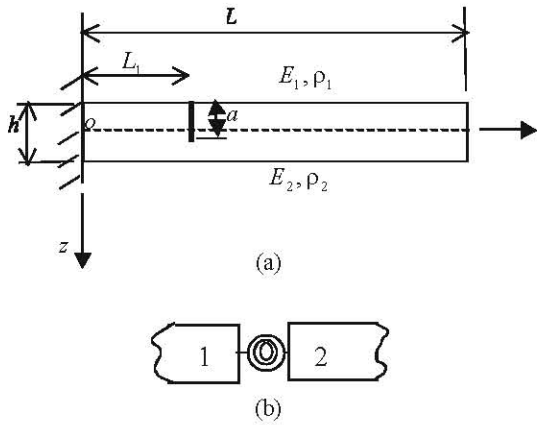

Fig. 1: (a) a FGM beam with an open edge crack; and (b) rotational spring model

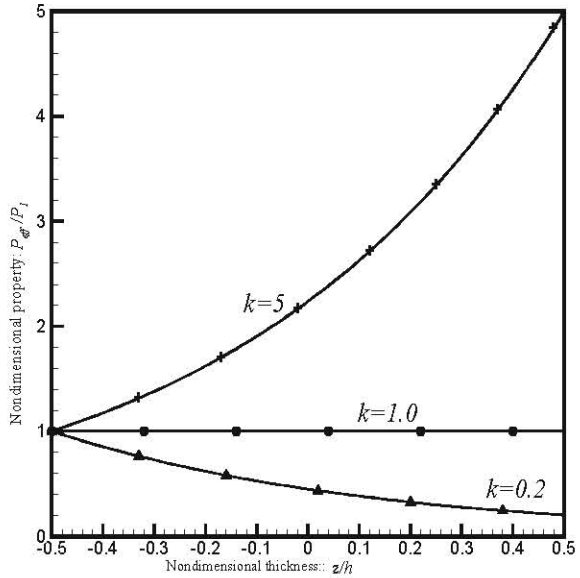

Fig. 2: The variation of material properties in an E-FGM beam

The Fgm Beam Model: A prismatic beam of length L and uniform thickness h with an edge crack of depth a located at a distance L_1 from the left end is considered as shown in Fig.1. Coordinates x defines the plane of the beam, whereas the z-axis originated at the middle surface of the beam is in the thickness direction. The material properties, Young's modulus and mass density, on the upper and lower surfaces are different but are preassigned according to the performance demands. The effect of Poisson's ratio on the deformation is much less than that of Young's modulus (Jin and Batra [18]). Thus, Poisson's ratio of the beams is assumed to be constant. The effective material properties P_{eff} in the thickness direction of the FGM beams vary with exponential functions (E-FGM) as follows.

$$P_{eff}(z) = P_1\sqrt{k}e^{z/h\,Ln(k)}, \quad \frac{-h}{2} \le z \le \frac{h}{2} \tag{1}$$

Where

$$\underline{k} = P_2 / P_1 \tag{2}$$

and P_1 and P_1 are material properties at the upper surface and lower surface of the FGM beam, respectively. P_{eff} in Eq. (1) is material properties corresponding to the modulus of elasticity and mass density. The material distribution in the thickness direction of the E-FGM beams is plotted in Fig. 2 which shows that the properties changes Ascensional for $k>1$ and changes descending for $k<1$. Also, Material properties are homogeneous and isotropic when $k=1$.

The Rotational Spring Model: It is assumed that the crack is perpendicular to the beam surface and always remains open. Based on the well accepted rotational-spring model, the cracked beam can be treated as two sub-beams connected by an elastic rotational spring at the cracked section which has no mass and no length. The bending stiffness of the cracked section K_T is related to the flexibility G by

$$K_T = \frac{1}{G} \tag{3}$$

From Broek's approximation [19], the flexibility of the beam G due to the presence of the crack can be derived as

$$\frac{1-\nu^2}{E(a)}(K_I)^2 = (\frac{M_I}{\sqrt{2}})^2\frac{dG}{da} \tag{4}$$

where M_I is the bending moment at the cracked section, K_I is the stress intensity factor (SIF) under mode I loading and is a function of the geometry, the loading and the material properties as well and $E(a)$ is Young's modulus at the crack tip

The formulas for the SIF as a function of the crack depth can be obtained from the data given by Erdogan and Wu [20] through Lagrange interpolation technique

$$K_I = \frac{6M_I\sqrt{\pi h\zeta}}{h^2}F(\zeta), \quad \zeta = \frac{a}{h}, \zeta \le 0.7 \tag{5}$$

where $\zeta \le 0.7$ implies that this paper considers crack depth ratio from 0.0 to 0.7 only and

$$F(\zeta)=395.919\zeta^7-971.767\zeta^6+1009.567\zeta^5-554.549\zeta^4+170.387\zeta^3-24.225\zeta^2+0.3\zeta+1.762 \quad \text{when } \frac{E_2}{E_1}=0.2 \tag{6-a}$$

$$F(\zeta)=-1031.750\zeta^7+2395.830\zeta^6-2124.310\zeta^5+909.375\zeta^4-192.451\zeta^3+21.667\zeta^2-1.662\zeta+1.150 \quad \text{when } \frac{E_2}{E_1}=1 \tag{6-b}$$

$$F(\zeta)=-122.978\zeta^7+296.701\zeta^6-249.533\zeta^5+94.003\zeta^4-12.567\zeta^3+0.860\zeta^2+0.300\zeta+0.605 \quad \text{when } \frac{E_2}{E_1}=5 \tag{6-c}$$

Substituting Eq. (5) into Eq. (4) leads to

$$G=\int_0^{\zeta}\frac{72\pi(1-\nu^2)\zeta F^2(\zeta)}{E(\zeta h)h^2}d\zeta \tag{7}$$

Kinematics and Constitutive Relations: The displacements of a material point located at (*x, z*) based on the Bernoulli-Euler beam theory is as the following form

$$u(x,y,z,t)=u_0(x,t)-z\frac{\partial w_0(x,t)}{\partial x},\ w(x,y,z,t)=w_0(x,t) \tag{8}$$

where u and w are the components of displacement along the *x*- and *z*- direction, respectively. Also, u_0 and w_0 are the displacements along the coordinate lines of a material point on the middle plane. The strain-displacement in terms of mid-plane deformation of Eq.(8) for a beam is

$$\varepsilon_{xx}=\varepsilon_{xx}^{o}+z\varepsilon_{xx}^{1} \tag{9}$$

where ε_{xx}^{o}, is the membrane strain,

$$\varepsilon_{xx}^{o}=\frac{\partial u_o}{\partial x} \tag{10}$$

and ε_{xx}^{1}, is the flexural (bending) strain,

$$\varepsilon_{xx}^{1}=-\frac{\partial^2 w_o}{\partial x^2} \tag{11}$$

The stress-strain relation of the functionally graded beam can be expressed as

$$\sigma_{xx}=E(z)\varepsilon_{xx} \tag{12}$$

Governing Equations: The governing equations and boundary conditions can be systematically derived via the Hamilton's principle as follows

$$\int_{t_1}^{t_2}(\delta T-\delta V)dt=0 \quad \delta u_o=\delta w_o=0 \qquad at \quad t=t_1,t \tag{13}$$

where δT and δV represent variation of kinetic energy and strain energy, respectively. These are defined as

Variation of kinetic energy:

$$\delta T=-\int_0^{L_1}\int_{-h/2}^{h/2}\rho(\ddot{u}\delta u+\ddot{w}\delta w)b\,dz\,dx-\int_{L_1}^{L}\int_{-h/2}^{h/2}\rho(\ddot{u}\delta u+\ddot{w}\delta w)b\,dz\,dx \tag{14}$$

Variation of strain energy:

$$\delta V=\int_0^{L_1}\int_{-h/2}^{h/2}(\sigma_{xx}\delta\varepsilon_{xx})b\,dz\,dx+\int_{L_1}^{L}\int_{-h/2}^{h/2}(\sigma_{xx}\delta\varepsilon_{xx})b\,dz\,dx+K_T\left(\frac{\partial w_o(L_1^+)}{\partial x}-\frac{\partial w_o(L_1^-)}{\partial x}\right) \tag{15}$$

where, dTdenotes the differential area element of middle plane of the beam and $\dot{(.)}=\frac{\partial}{\partial t}(.)$. Substituting Eqs. (14,15) into Eq. (13), using the integration by part and noting the fact that the variations (δu_0, δw_0) are independent and arbitrary, the equations of motion and the related boundary conditions can be obtained as

$$\delta u_{oi}:\frac{\partial N_{xxi}}{\partial x}=I_1\ddot{u}_{oi}-I_2\frac{\partial\ddot{w}_{oi}}{\partial x} \tag{16}$$

$$\delta w_{oi}:\frac{\partial^2 M_{xxi}}{\partial x^2}=I_1\ddot{w}_{oi}+\frac{\partial}{\partial x}(I_2\ddot{u}_{oi}-I_3\frac{\partial\ddot{w}_{oi}}{\partial x}) \tag{17}$$

By ignoring the in-plane inertia and rotary inertial effects, the equations (16) and (17) are reduced to

$$\delta u_{oi} : \frac{\partial N_{xxi}}{\partial x} = 0 \tag{18}$$

$$\delta w_{oi} : \frac{\partial^2 M_{xxi}}{\partial x^2} = I_1 \ddot{w}_{oi} \tag{19}$$

where subscript $i = 1$ and $i = 2$ refer to the left sub-beam and right sub-beam, respectively, divided by the crack. Also the boundary conditions for a cantilevered FGM beam are as

at $x = 0$

$$u_O = 0, w_O = 0 \frac{\partial w_O}{\partial x} = 0 \tag{20-a}$$

at x =L

$$N_{xx} = 0, M_{xx} = 0, \frac{\partial M_{xx}}{\partial x} = 0 \tag{20-b}$$

at $x = L_1$

$$u_{O1} = u_{O2}, w_{O1} = w_{O2}, N_{xx1} = N_{xx2} \tag{20-c}$$

$$M_{xx1} = M_{xx2}, \frac{\partial M_{xx1}}{\partial x} = \frac{\partial M_{xx2}}{\partial x}, K_T \frac{dw_{O1}}{dx} - M_{xx1} = K_T \frac{dw_{O2}}{dx}$$

The stress resultant N_{xx} which is force per unit length and the stress moment M_{xx} which is moments per unit length, are defined from the following integral expressions

$$N_{xx} = \int_{-h/2}^{h/2} \sigma_{xx} dz, M_{xx} = \int_{-h/2}^{h/2} z\sigma_{xx} dz \tag{21}$$

I_i (i = 1,2,3) are the mass inertia terms defined as

$$(I_1, I_2, I_3) = \int_{-h/2}^{h/2} \rho(z)(1, z, z^2) dz \tag{22}$$

By using the strain-displacement Eq.(9) and the stress-strain Eq.(12), the stress force and moment resultants, which are defined in Eq. (21), can be explained as

$$N_{xx} = A_{11}\varepsilon_{xx}^{o} + B_{11}\varepsilon_{xx}^{1}, M_{xx} = B_{11}\varepsilon_{xx}^{o} + D_{11}\varepsilon_{xx}^{1} \tag{23}$$

where A_{11}, B_{11} and D_{11}, are the in-plane, bending-stretching coupling and bending stiffness respectively, as

$$(A_{11}, B_{11}, D_{11}) = \int_{-h/2}^{h/2} E(z)(1, z, z^2) dz \tag{24}$$

Substituting Eq. (23,10,11) into Eqs. (18,19) and some simplification leads to the following governing equation

$$\delta u_{oi} : A_{11} \frac{\partial^2 u_{oi}}{\partial x^2} - B_{11} \frac{\partial^3 w_{oi}}{\partial x^3} = 0, \delta w_{oi} : (D_{11} - \frac{B_{11}^2}{A_{11}}) \frac{\partial^4 w_{oi}}{\partial x^4} + I_1 \ddot{w}_{oi} = 0 \tag{25-a,b}$$

Solution of the Differential Equation: For harmonic vibrations, the displacements can be expressed as

$$u_{oi}(x,t) = U_{oi}(x)e^{i\omega t}, w_{oi}, w_{oi}(x,t) = W_{oi}(x)e^{i\omega t}, i = 1,2 \tag{26}$$

where ω is the natural frequency of the cracked FGM beam. Substitution of Eq. (26) into Eq. (25-b) leads to the deflection solution

$$W_{oi} = e_{i1}\sin(\lambda x) + e_{i2}\cos(\lambda x) + e_{i3}\sinh(\lambda x) + e_{i4}\cosh(\lambda x) \tag{27}$$

Where

$$\lambda = \sqrt[4]{\frac{I_1\omega^2}{d}} \qquad ,d = (D_{11} - \frac{B_{11}^2}{A_{11}}) \tag{28}$$

The axial displacement $U_i(x)$ can then be obtained from Eq. (25-a) as

$$U_{oi} = \lambda \frac{B_{11}}{A_{11}}[e_{i1}\cos(\lambda x) - e_{i2}\sin(\lambda x) + e_{i3}\cosh(\lambda x) + e_{i4}\sinh(\lambda x)] + g_i x + g_{i0}, i = 1,2 \tag{29}$$

Substitution of equation (27, 29) into (20) will yield the characteristic equation of the FGM cracked beam:

$$[H]\ \{q\} = \{10\} \tag{30}$$

where

$$\{q\} = \{e_{11}\ e_{12}\ \ e_{13}\ \ e_{14}\ g_1\ g_{10}\ \ e_{21}\ \ e_{22}\ \ e_{23}\ \ e_{24}\ g_2\ g_{20}\}^T \tag{31}$$

and $[H]$ the 12×12 characteristic matrix being the function of frequency.

Solving for $([H(\lambda] = 0$ yields the natural frequencies. Substituting each natural frequency back into equation (30) will give the corresponding mode shape. Note that both the natural frequency and the mode shape now depend not only on the crack depth and location, but also on the material. The characteristic matrix$[H]$ is given as

$$\begin{bmatrix}
0 & 0 & 0 & 0 & 0 & 1 & 0 & 0 & 0 & 0 & 0 & 0 \\
0 & 1 & 0 & 1 & 0 & 0 & 0 & 0 & 0 & 0 & 0 & 0 \\
1 & 0 & 1 & 0 & 0 & 0 & 0 & 0 & 0 & 0 & 0 & 0 \\
0 & 0 & 0 & 0 & 0 & 0 & 0 & 0 & 0 & 0 & 1 & 0 \\
0 & 0 & 0 & 0 & 0 & 0 & J_{10} & J_{20} & -J_{30} & -J_{40} & \frac{B_{11}}{d\lambda^2} & 0 \\
0 & 0 & 0 & 0 & 0 & 0 & -J_{20} & J_{10} & J_{40} & J_{30} & 0 & 0 \\
\frac{\lambda B_{11}}{A_{11}}J_{21} & -\frac{\lambda B_{11}}{A_{11}}J_{11} & \frac{\lambda B_{11}}{A_{11}}J_{41} & \frac{\lambda B_{11}}{A_{11}}J_{31} & L_1 & 1 & -\frac{\lambda B_{11}}{A_{11}}J_{21} & \frac{\lambda B_{11}}{A_{11}}J_{11} & -\frac{\lambda B_{11}}{A_{11}}J_{41} & -\frac{\lambda B_{11}}{A_{11}}J_{31} & -L_1 & -1 \\
J_{11} & J_{21} & J_{31} & J_{41} & 0 & 0 & -J_{11} & -J_{21} & -J_{31} & -J_{41} & 0 & 0 \\
0 & 0 & 0 & 0 & 1 & 0 & 0 & 0 & 0 & 0 & -1 & 0 \\
-J_{11} & -J_{21} & J_{31} & J_{41} & -\frac{B_{11}}{d\lambda^2} & 0 & J_{11} & J_{21} & -J_{31} & -J_{41} & \frac{B_{11}}{d\lambda^2} & 0 \\
-J_{21} & J_{11} & J_{41} & J_{31} & 0 & 0 & J_{21} & -J_{11} & -J_{41} & -J_{31} & 0 & 0 \\
J_{21} - \frac{\lambda d}{K_T}J_{11} & -J_{11} - \frac{\lambda d}{K_T}J_{21} & J_{41} + \frac{\lambda d}{K_T}J_{31} & J_{31} + \frac{\lambda d}{K_T}J_{41} & \frac{-B_{11}}{K_T\lambda} & 0 & -J_{21} & J_{11} & -J_{41} & -J_{31} & 0 & 0
\end{bmatrix} \tag{32}$$

where

$$J_{10} = \sin(\lambda L), J_{20} = \sin(\lambda L), J_{30} = \sin(\lambda L), J_{40} = \sin(\lambda L),$$
$$J_{11} = \sin(\lambda L), J_{11} = \sin(\lambda L), J_{31} = \sin(\lambda L), J_{41} = \sin(\lambda L),$$

Numerical Results and Discussions: Unless otherwise stated, it is assumed the considered FGM cantilever beam has the following geometric and material parameters

$$h = 0.1m, \frac{L}{h} = 20, E_1 = 70GPa, \nu = 0.33, \rho = 2780\ kg/m^3 \tag{33}$$

Table 1 gives the fundamental frequency ratio $\frac{\omega_1}{\omega_{1O}}$ of a cracked cantilevered isotropic beam $(\frac{L}{h} = 4.0, \nu = 0.3, \frac{a}{h} = 0.2)$ at different locations. This example was previously analyzed by Yokoyama and Chen [9] using the finite element method and Bernoulli-Euler beam theory. Our analytical solutions are in good agreement with the finite element results.

Table 1: Fundamental frequency ratio $\frac{\omega_1}{\omega_{1o}}$ of an isotropic homogenous cantilevered beam $(\frac{L}{h}=4.0, \nu=0.3, \frac{a}{h}=0.2)$

$\frac{L_1}{L}=0.2$		$\frac{L_1}{L}=0.4$		$\frac{L_1}{L}=0.6$	
Yokoyama and Chen[9]	Present	Yokoyama and Chen[9]	Present	Yokoyama and Chen[9]	Present
0.94101	0.96556	0.96667	0.98563	0.99583	0.99637

Table 2: First three dimensionless natural frequencies of intact FGM cantilevered beams $(E_1=70GPa, \nu=0.33, \rho=2780\ kg/m^3)$

		$\bar{\omega}_1$		$\bar{\omega}_2$		$\bar{\omega}_3$	
$\frac{L}{h}$	$\frac{E_2}{E_1}$	Yu and Chu p-FEM[21]	Present	Yu and Chu p-FEM[21]	Present	Yu and Chu p-FEM[21]	Present
20	0.2	0.83	0.83	5.18	5.18	14.49	14.49
	1	0.88	0.88	5.51	5.51	15.42	15.42
	5	0.83	0.83	5.18	5.18	14.49	14.49
10	0.2	3.3	3.3	20.7	20.7	57.97	57.97
	1	3.52	3.52	22.03	22.03	61.7	61.7
	5	3.3	3.3	20.7	20.7	57.97	57.97

In Table 2, the lowest three modal frequencies of the intact FGM cantilevered beam are calculated by the present method and are compared with those reported by Yu and Chu [21]. In their work the p-FEM was used for calculation of frequencies and the modal frequencies were normalized as

$$\bar{\omega}_n = \frac{\omega_n}{\sqrt{d_o / I_o}} \tag{34}$$

Where d_0 and I_0 are the corresponding values of d and I_0 of an isotropic homogeneous beam $(\frac{E_2}{E_1}=1)$.

Figures. 3-11 present analytical solutions for the free vibration of cantilevered functionally graded beams containing an open edge crack.

Figure 3 shows the fundamental frequency ratio $\frac{\omega_1}{\omega_{1o}}$ of various FGM cracked beams versus crack location for various material gradient and crack depth. The frequency ratio also tends to be considerably lower as the Young's modulus ratio E_2 / E_1 decreases from 5.0 to 0.2, in other words, the natural frequencies of FGM beams with weaker bending stiffness are more sensitive to the crack. The frequency ratio is the minimum when the crack is located at the fixed end of the beam where the maximum bending moment under a uniformly distributed load is achieved.

The results for the 2nd and 3rd frequencies are demonstrated in Fig. 4 and Fig. 5, respectively. It seems to be much more complicated than those for the fundamental frequency. Additionally, a fact that may be derived from the figures is that when the crack located at certain positions, the natural frequencies of the second mode or the higher modes keep unchanged. These positions are usually called vibration nodes for a given mode.

The first three natural frequency ratios as functions of crack depth for different crack locations and material gradients are shown in Figs. 6-8. As indicated from these figures, the first three natural frequency ratios vary with the normalized crack size. For a certain normalized crack location and material gradient, the first three frequency ratios would monotonically decrease as the crack size increases. It can be derived from the fact the crack would introduce local flexibility and then lead to loss of structural stiffness.

The first three mode shapes of cantilevered FGM beams ($E_2 / E_1 = 5$) correspond to the first three natural frequency with an open edge crack of various crack depths ($a / h = 0.1, 0.3, 0.5, 0.7$) are compared in Figs. 9-11. As can be observed, the mode shapes of bending deflection w of the cracked beam are changed due to the crack. It can be clearly seen from these figures that an open edge crack leads to discontinuity in bending slope at the crack location.

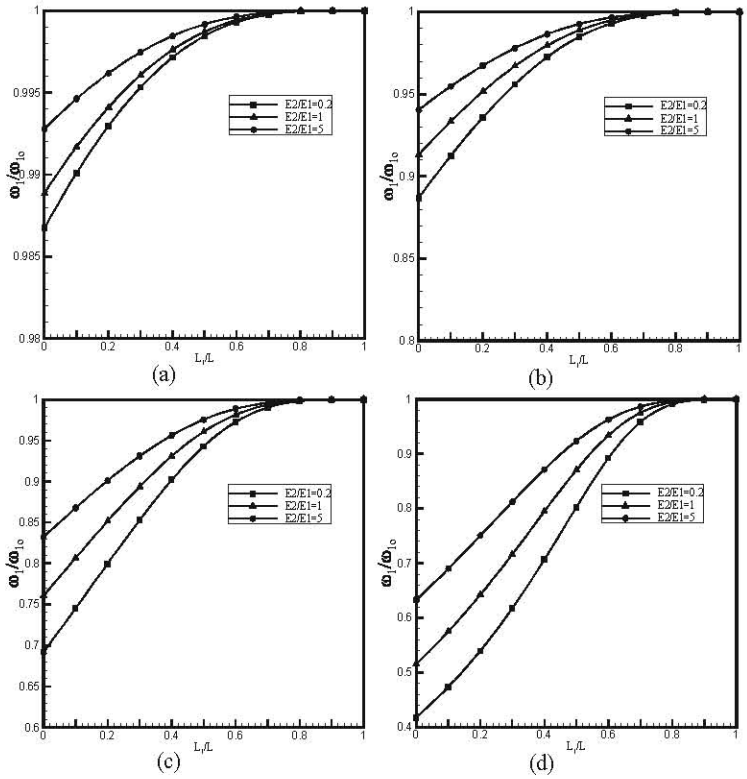

Fig. 3: Fundamental frequency ratio of FGM cracked beams verses crack locations and varying material gradient and crack depth: (a) $a / h = 0.1$, (b) $a / h = 0.3$, (c) $a / h = 0.5$, (d) $a / h = 0.7$,

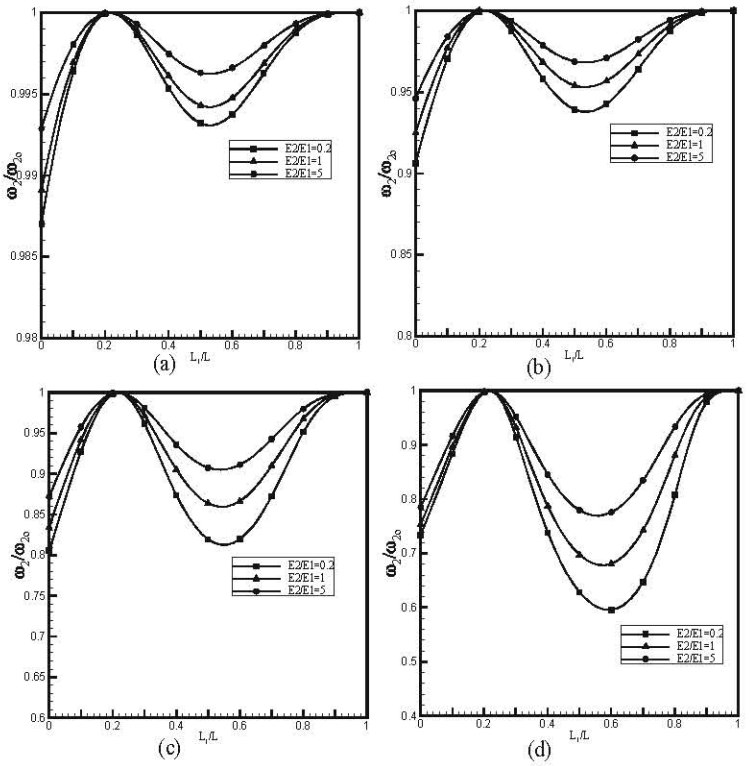

Fig. 4: The 2nd frequency ratios of FGM cracked beams verses crack locations and varying material gradient and crack depth:(a) $a / h = 0.1$, (b) $a / h = 0.3$, (c) $a / h = 0.5$, (d) $a / h = 0.7$,

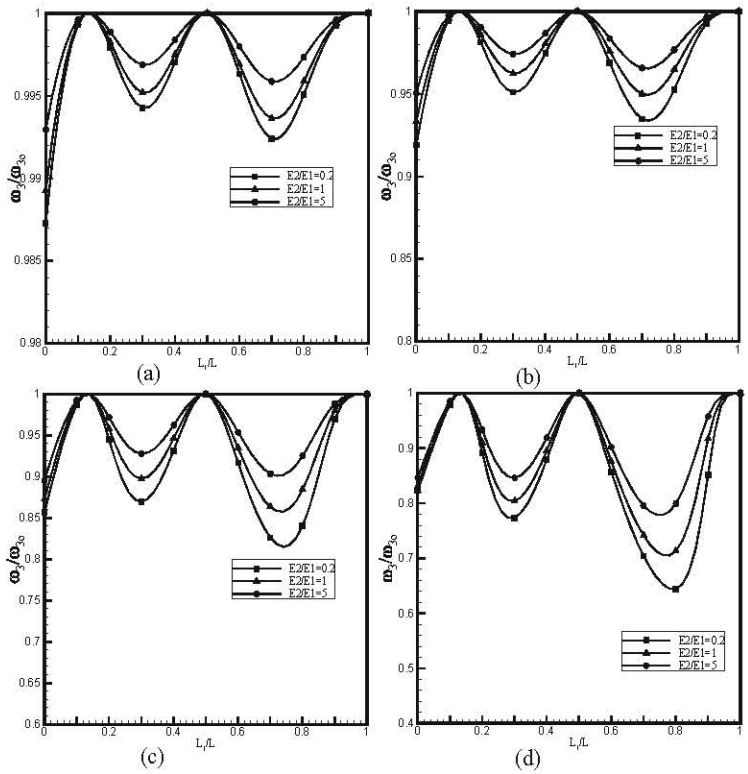

Fig. 5: The 3rd frequency ratios of FGM cracked beams verses crack locations and varying material gradient and crack depth: (a) $a / h = 0.1$, (b) $a / h = 0.3$, (c) $a / h = 0.5$, (d) $a / h = 0.7$,

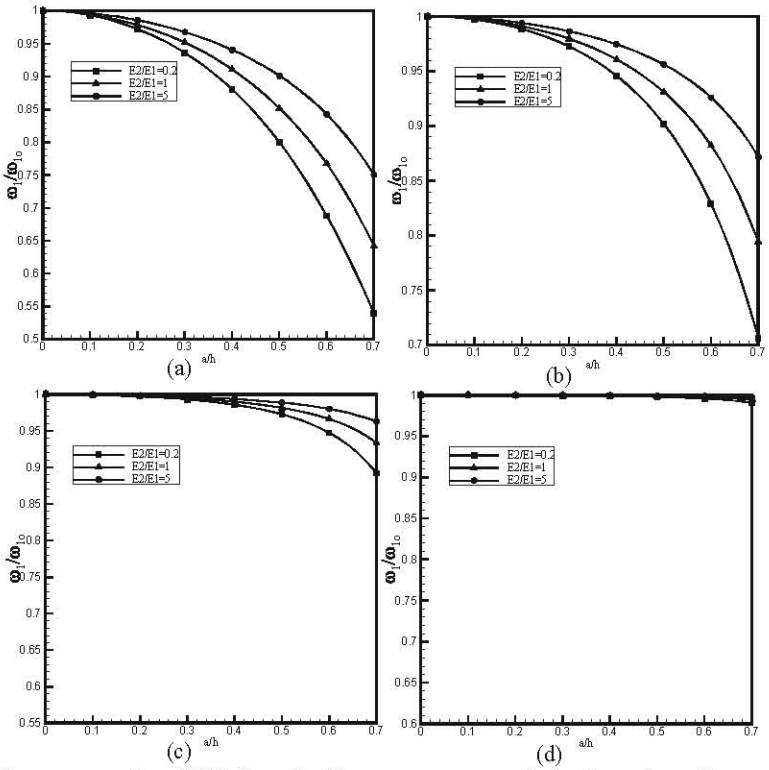

Fig. 6: Fundamental frequency ratio of FGM cracked beams verses crack depth and varying material gradient and crack location:(a) $L_1 / L = 0.2$, (b) $L_1 / L = 0.4$, (c) $L_1 / L = 0.6$, (d) $L_1 / L = 0.8$,

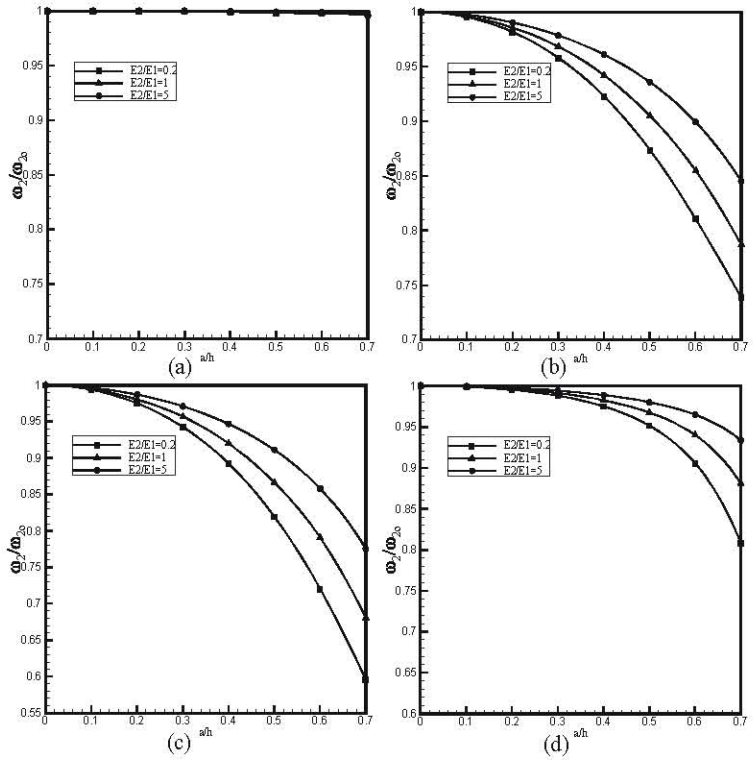

Fig. 7: 2nd frequency ratio of FGM cracked beams verses crack depth and varying material gradient and crack location:(a) $L_1 / L = 0.2$, (b) $L_1 / L = 0.4$, (c) $L_1 / L = 0.6$, (d) $L_1 / L = 0.8$,

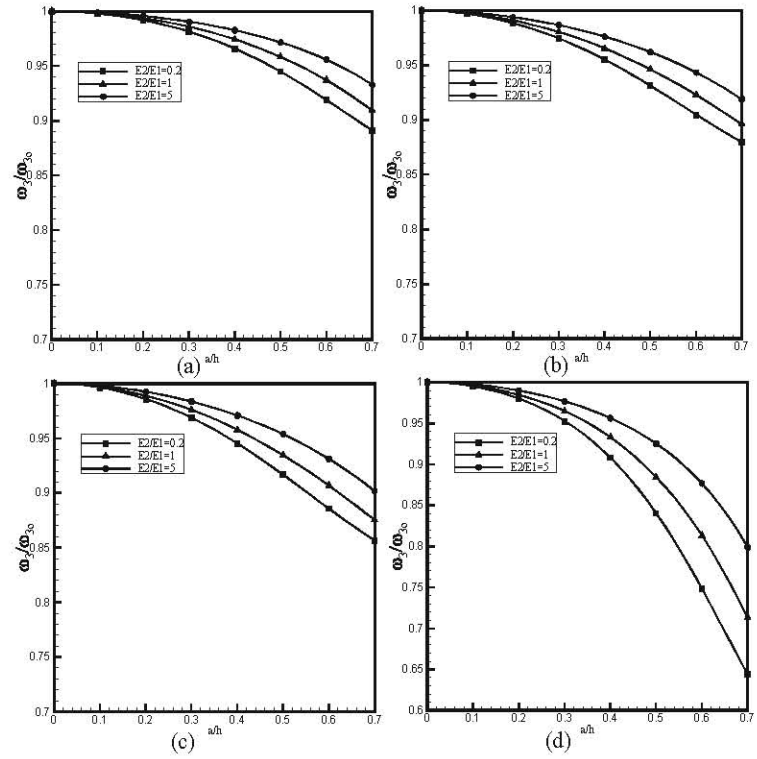

Fig. 8: 3rd frequency ratio of FGM cracked beams verses crack depth and varying material gradient and crack location: (a) $L_1 / L = 0.2$, (b) $L_1 / L = 0.4$, (c) $L_1 / L = 0.6$, (d) $L_1 / L = 0.8$,

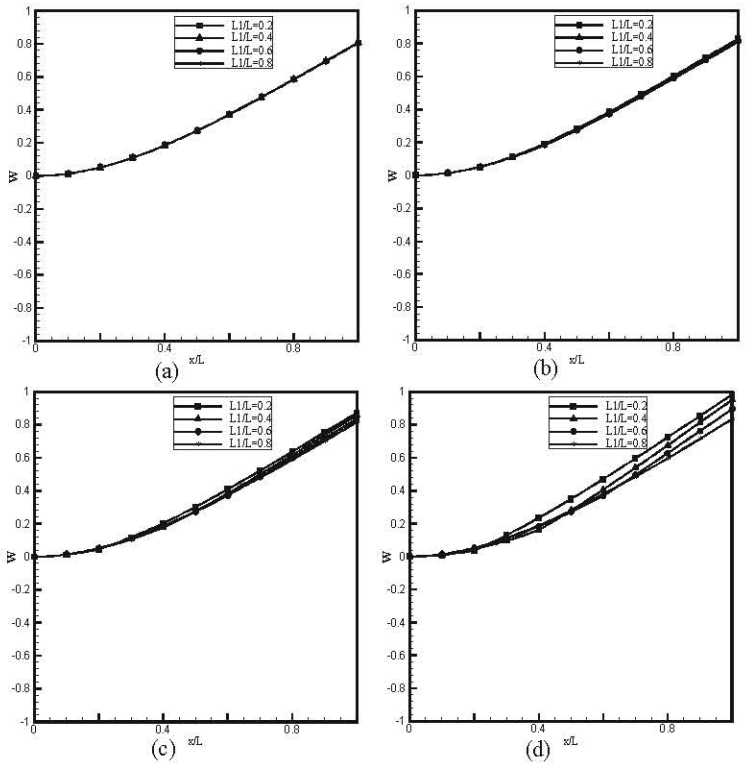

Fig. 9: First mode shape of FGM cracked beams with different crack depths and crack locations ($\frac{E_2}{E_1} = 5$) .(a) $a / h = 0.1$, (b) $a / h = 0.3$, (c) $a / h = 0.5$, (d) $a / h = 0.7$,

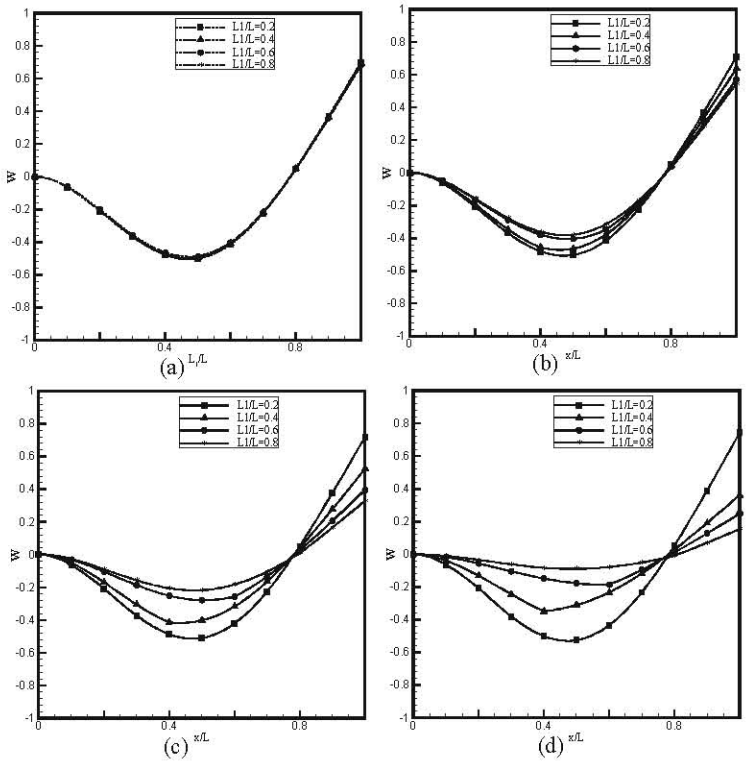

Fig. 10: 2nd mode shape of FGM cracked beams with different crack depths and crack locations ($\frac{E_2}{E_1} = 5$) .(a) $a / h = 0.1$, (b) $a / h = 0.3$, (c) $a / h = 0.5$, (d) $a / h = 0.7$,

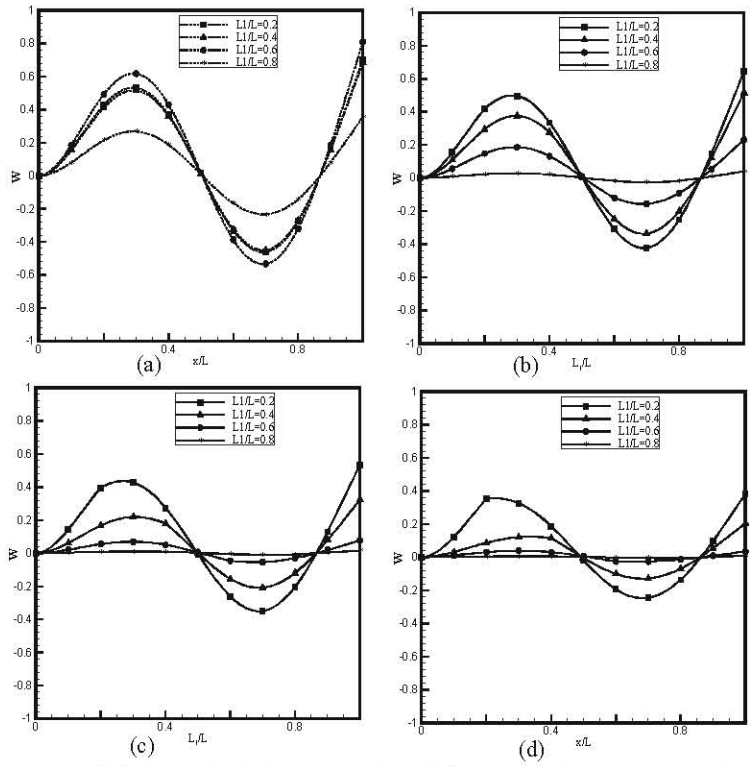

Fig. 11: 3rd mode shape of FGM cracked beams with different crack depths and crack locations $(\frac{E_2}{E_1} = 5)$. (a) $a/h = 0.1$, (b) $a/h = 0.3$, (c) $a/h = 0.5$, (d) $a/h = 0.7$,

CONCLUSIONS

Free vibration of functionally graded cantilevered beams with an open edge crack is theoretically investigated in this paper by using the analytical approach based on the rotational-spring model. A parametric study has been conducted to discuss the effects of the crack location and material gradient on both the natural frequencies and the corresponding mode shapes of cracked FGM beams. The vibration behavior of a FGM beam with a lower Young's modulus ratio E_2/E_1 is more sensitive to the presence of cracks. Also, the fundamental frequency ratio become much lower as the crack is located near where the maximum bending moment due to a uniform distributed load occurs. The frequency ratios would monotonically decrease as the crack size increases. It is due to the presence of the crack which would introduce local flexibility and then lead to loss of structural stiffness.

REFERENCES

1. Kirshmer, P.G., 1944. The effect of discontinuities on the natural frequency of beams. Proceedings of the American Society of Testing and Materials, 44: 897-904.
2. Thomson, W.J., 1943. Vibration of slender bars with discontinuities in stiffness. J. Applied Mechanics, 17: 203-207.
3. Petroski, H.J., 1981. Simple static and dynamic models for the cracked elastic beam. International J. Fracture, 17: R71-R76.
4. Petroski, H.J., 1983. Structural dynamics of piping with stable cracks; some simple models. International J. Pressure Vessels and Piping, 13: 1-18.
5. Dimarogonas, A.D., 1976. Vibration Engineering. St. Paul, Minnesota, West. Publishers.
6. Chondros, T., 1977. Dynamic response of cracked beams. M.Sc. Thesis, University of Patras, Greece.
7. Chondros, T.G. and A.D. Dimarogonas, 1980. Identification of cracks in welded joints of complex structures. J. Sound and Vibration, 69: 531-538.
8. Chondros, T.G. and A.D. Dimarogonas, 1979. Identification of cracks in circular plates welded at the contour. American Society of Mechanical Engineers Design Engineering Technical Conference, St. Louis, pp: 79-DET-106.
9. Yokoyama, T. and M.C. Chen, 1998. Vibration analysis of edge-cracked beams using a line-spring model. Engineering Fracture Mechanics, 59(3): 403-9.

10. Hsu, M.H., 2005. Vibration analysis of edge-cracked beam on elastic foundation with axial loading using the differential quadrature method. Computer Methods in Applied Mechanics and Engineering, 194(1): 1-17.
11. Rizos, P.F., N. Aspragathos and A.D. Dimarogonas, 1990. Identification of crack location and magnitude in a cantilever beam from the vibration modes. J. Sound and Vibration, 138(3): 381-388,
12. Narkis, 1994. Identification of crack location in vibrating simply supported beams. J. Sound and Vibration, 172: 549-558.
13. Sankar, B.V. and J.T. Tzeng, 2002. Thermal Stresses in Functionally Graded Beams, AIAA J., 40(6): 1228-1232.
14. Wu, L., Q.S. Wang and I. Elishakoff, 2005. Semi-inverse method for axially functionally graded beams with an anti-symmetric vibration mode. J. Sound and Vibration, 284: 1190-202.
15. Librescu, L., S.Y. Oh and O. Song, 2005. Spinning thin-walled beams made of functionally graded materials and operating in a high temperature environment: Vibration and instability. J. Thermal Stresses, 28: 694-712.
16. Xiang, H.J. and J. Yang, 2008. Free and forced vibration of a laminated FGM Timoshenko beam of variable thickness under heat conduction. Composites: Part. B., 39: 292-303.
17. Simsek, M. and T. Kocatürk, 2009. Free and forced vibration of a functionally graded beam subjected to a concentrated moving harmonic load, Composite Structures, 90: 465-473.
18. Jin, Z.H. and R.C. Batra, 1996. Stress Intensity Relaxation at the Tip of an Edge Crack in a Functionally Graded Material Subjected to a Thermal Shock. J. Thermal Stresses, 19: 317-339.
19. Broek, D., 1986. Elementary Engineering Fracture Mechanics. Martinus Nijhoff.
20. Erdogan, F. and B.H. Wu, 1997. The Surface Crack Problem for a Plate with Functionally Graded Properties. J. Applied Mechanics, 64: 448-456.
21. Yu, Z. and F. Chu, 2009. Identification of crack in functionally graded material beams using the p-version of finite element method. Journal of Sound and Vibration, 325: 69-84.